

Coherent-potential-approximation study of excitonic absorption in orientationally disordered molecular aggregates

D.B. Balagurov* and G.C. La Rocca

Scuola Normale Superiore and INFM, Piazza dei Cavalieri 7, 56126 Pisa, Italy

V.M. Agranovich

Institute of Spectroscopy, Russian Academy of Sciences, 142190 Troitsk, Moscow Region, Russia

We study the dynamics of a single Frenkel exciton in a disordered molecular chain. The coherent-potential approximation (CPA) is applied to the situation when the single-molecule excitation energies as well as the transition dipole moments, both their absolute values and orientations, are random. Such model is believed to be relevant for the description of the linear optical properties of one-dimensional J aggregates. We calculate the exciton density of states, the linear absorption spectra and the exciton coherence length which reveals itself in the linear optics. A detailed analysis of the low-disorder limit of the theory is presented. In particular, we derive asymptotic formulas relating the absorption linewidth and the exciton coherence length to the strength of disorder. Such expressions account simultaneously for all the above types of disorder and reduce to well-established form when no disorder in the transition dipoles is present. The theory is applied to the case of purely orientational disorder and is shown to agree well with exact numerical diagonalization.

PACS numbers: 71.35.Aa; 78.30.Ly

I. INTRODUCTION

The optically active states in organic molecular aggregates^{1,2} — the spatially-regular linear arrangements of dye molecules — are one-dimensional Frenkel excitons.³ The nature of the excitonic states to be extended over many molecules reveals itself in the narrowing of the absorption resonances and the shortening of the radiative lifetime upon aggregate formation (effects known as exchange narrowing and “superradiance”).⁴ The related coherence length coincides with the total number of molecules in the aggregate only if the size of the latter is sufficiently small. Otherwise various exciton decoherence mechanisms, among which the static disorder is the most essential at low temperature, substantially reduce the coherence length that becomes independent from the actual size of the aggregate. Considerable work has been done to analyze the aspects of disorder in the molecular excitation energies^{4,5,6,7,8,9,10,11} and positions.^{12,13,14,15,16} Much less attention has been devoted to the disorder in orientations¹⁷ or, generally, in the transition dipole moments of individual molecules. However, from the limited available information on the actual structure of molecular arrangements one cannot exclude that the transition dipoles are seriously influenced by disorder. Moreover, the last type of disorder affects in a nontrivial way the separate components of the optical susceptibility tensor and, hence, would be observable in polarization-resolved absorption and luminescence experiments¹⁸. The present work has been motivated by the need for a detailed theoretical analysis of orientational disorder, as well as clarification of certain aspects concerning the exciton coherence length in molecular aggregates.

In this paper the linear optical properties of a disordered molecular chain are studied using the single-site

coherent-potential approximation^{19,20} (CPA). Applied to various disorder problems, such as that of the electronic structure in a random alloy, this self-consistent approximation was shown to reproduce well the single-particle characteristics like the density of states (DOS). As for the systems in which elementary excitations are Frenkel excitons, the CPA is in addition capable to provide the complete information on the linear optical response, because the latter is extracted only from the single-exciton Green’s function (GF) averaged over disorder realizations. The CPA has been successfully used to model the optical spectra of periodic molecular arrangements with random on-site energies^{21,22} and composition.²³ However, if the transition dipoles are also affected by disorder, a proper modification of the theory is required. The key observation which allows us to do this is that the dipoles enter the off-diagonal part of the Hamiltonian in a bilinear form. In this case a single-site approximation can be constructed according to a vector analog of the Shiba ansatz.²⁴ The resulting scheme is equivalent to the matrix extension of CPA derived by Blackman, Esterling and Berk²⁵ (BEB) for compositionally-disordered alloys with random hopping energies. [The analytical properties of BEB CPA have been examined in Refs. 26,27,28,29]. Persson and Liebsch³⁰, and Rozenbaum *et al.*³¹ have constructed a similar version of CPA to study, respectively, the susceptibility of polarizable particles and the vibrational modes of coupled oscillators randomly and isotropically oriented in two or three dimensions. However, their theory is still not applicable to the molecular aggregates in which one typically deals with an essentially anisotropic distribution of the transition dipoles.

The paper is organized as follows. In the next section we define the model of a disordered molecular aggregate and set up the basic formalism for the forthcoming cal-

culations. The exciton Green's tensor is introduced to express the related single-particle quantities: the DOS, the linear polarizability, and the coherence length. In Sec. III we present the general formulation of the BEB-CPA scheme and in Sec. IV derive its analytic solution in the low-disorder limit. In Sec. V the theory is applied to a specific case of orientational disorder and compared to the results of the exact numerical diagonalization.

II. BASIC FORMALISM

A. Model

An aggregate can be considered as a chain of \mathcal{N} identical two-level molecules. The linear optical properties in the resonance region are determined by the single-particle states of the Frenkel Hamiltonian³

$$H = \sum_n \epsilon_n B_n^\dagger B_n + \sum_{n,m} J_{nm} B_n^\dagger B_m. \quad (1)$$

The operator B_n^\dagger (B_n) creates (annihilates) an electronic excitation of energy ϵ_n on the n th molecule (whose excited state is supposed to be nondegenerate). The transfer terms J_{nm} result from the Coulomb interaction between an excited molecule and one in the ground state. Accounting only for the dipole-dipole contribution one has

$$J_{nm} = \sum_{\alpha,\beta} p_n^\alpha \vartheta_{nm}^{\alpha\beta} p_m^\beta, \quad (2)$$

where p_n^α are the vector components of the n th molecule transition dipole. The “coupling kernel” $\vartheta_{nm}^{\alpha\beta}$ carries information on the dielectric function of the surrounding material and the location of the molecules, but not on their dipole moments. If the dynamics of the exciton subsystem is nondissipative (and the molecules have no magnetic structure, so that p_n^α can be chosen real) $\vartheta_{nm}^{\alpha\beta}$ has to be symmetric in the tensorial indices ($\vartheta_{nm}^{\alpha\beta} = \vartheta_{nm}^{\beta\alpha}$). We shall assume the molecules to form a one-dimensional regular lattice such that $\vartheta_{nm}^{\alpha\beta}$ depends solely on the intermolecular distance $|n - m|$ (measured in the units of lattice spacing). The theory will be presented in a general way without specifying a concrete form of this dependence, i.e., for any screening and anisotropy of the Coulomb interaction that can occur in a solvent or on a substrate interface.

The disorder enters in our model both through the on-site energies ϵ_n and the dipole moments p_n^α . We shall assume the families of random parameters $\{\epsilon_n, p_n^\alpha\}$ corresponding to distinct sites to be mutually independent and to have identical probability distribution. At the same time we still allow for correlations between the transition energy and the dipole components of a given molecule.

Finally, we shall neglect everywhere the effects of a finite length of the aggregate considering the limit $\mathcal{N} \rightarrow \infty$. This approximation is justified for sufficiently strong

disorder when the exciton coherence length found for the infinite system does not exceed the actual length of the chain.

B. Exciton Green's tensor

For a given random realization the total information on the aggregate's optical dynamics is imbedded in the complete set of single-exciton eigenstates $\sum_n \psi_n(E) B_n^\dagger |0\rangle$; the vacuum $|0\rangle$ is the direct product of the molecular ground states; $\psi_n(E)$ is the real-space exciton wave function with an eigenenergy E . The local density of states (LDOS) on the n th site and the total (normalized) exciton DOS are found as

$$\rho_n(\omega) = \sum_{\{E\}} |\psi_n(E)|^2 \delta(\omega - E) = -\frac{1}{\pi} \text{Im} G_{nn}(\omega), \quad (3)$$

$$\rho(\omega) = \frac{1}{\mathcal{N}} \sum_{\{E\}} \delta(\omega - E) = -\frac{1}{\pi \mathcal{N}} \sum_n \text{Im} G_{nn}(\omega), \quad (4)$$

where the real-space single-exciton GF is given by

$$G_{nm}(z) = -i \int_0^{+\infty} dt e^{izt} \langle 0 | B_n(t) B_m^\dagger(0) | 0 \rangle \\ = \sum_{\{E\}} \frac{\psi_n(E) \psi_m^*(E)}{z - E} \quad (5)$$

and the symbol $\{E\}$ indicates that summation is performed over all eigenstates. Here and below the GF for a real-valued argument ω is found as the limit $z \rightarrow \omega + i0^+$. Assuming that around the single-exciton resonance the light wavelength is much larger than the spatial extent of a typical excitonic wave function the aggregate interacts with the optical field as a pointlike dipole. Hence, the linear response to the external optical field is completely described by the polarizability tensor

$$\chi^{\alpha\beta}(z) = i \int_0^{+\infty} dt e^{izt} \langle 0 | [P^\alpha(t), P^\beta(0)] | 0 \rangle. \quad (6)$$

in which the operator of total polarization represents the sum of local polarizations, $P^\alpha = \sum_n (P_n^{\alpha(+)} + P_n^{\alpha(-)})$, both positive- and negative-energy components:

$$P_n^{\alpha(+)} = p_n^\alpha B_n^\dagger, \quad P_n^{\alpha(-)} = p_n^\alpha B_n. \quad (7)$$

To set up a convenient formalism for the forthcoming discussion let us define the time-ordered two-point correlator of the local polarizations

$$\Gamma_{nm}^{\alpha\beta}(z) = -i \int_0^{+\infty} dt e^{izt} \langle 0 | P_n^{\alpha(-)}(t) P_m^{\beta(+)}(0) | 0 \rangle, \quad (8)$$

or, equivalently,

$$\Gamma_{nm}^{\alpha\beta}(z) = p_n^\alpha G_{nm}(z) p_m^\beta. \quad (9)$$

The newly introduced quantity will be referred through the paper as the Green's tensor (GT), as opposed to the “scalar” GF considered above. Combining the previous formulas we arrive at the straightforward relation

$$\chi^{\alpha\beta}(z) = - \sum_{n,m} [\Gamma_{nm}^{\alpha\beta}(z) + \Gamma_{nm}^{\alpha\beta*}(-z^*)], \quad (10)$$

which indicates that (up to the sign factor) the GT coincides with the positive-energy counterpart of the local linear response function.

As usual one is interested not in the solution of the entire dynamical problem for a given disorder realization, but in finding the configurational average of some basic observable parameters. In our case the quantities of interest are those defined in Eqs. (4) and (10). The subsequent implementation of CPA suggests that the disorder-averaged DOS $\bar{\rho}(\omega) \equiv \langle \rho(\omega) \rangle$ and polarizability $\bar{\chi}^{\alpha\beta}(z) \equiv \langle \chi^{\alpha\beta}(z) \rangle$ are to be expressed in terms of the conditionally-averaged on-site GT

$$\tilde{\Gamma}_{nn}^{\alpha\beta}(z) \equiv \langle \Gamma_{nn}^{\alpha\beta}(z) \rangle_{\text{all sites except } n\text{th}}, \quad (11)$$

with fixed n th site variables $\{\epsilon_n, p_n^\alpha\}$, and the complete statistical average

$$\bar{\Gamma}_{nm}^{\alpha\beta}(z) \equiv \langle \Gamma_{nm}^{\alpha\beta}(z) \rangle, \quad (12)$$

the only quantities accessible within a single-site effective theory. To proceed with the DOS it is sufficient to notice that, because the n th-site dipoles p_n^α remain fixed, the conditional average of the local GT and GF are still related to each other as established in Eq. (9), $\tilde{\Gamma}_{nn}^{\alpha\beta}(z) = p_n^\alpha \tilde{G}_{nn}(z) p_n^\beta$. As a result the scalar GF is obtained via projection

$$\tilde{G}_{nn}(z) = \sum_{\alpha,\beta} \frac{p_n^\alpha}{|p_n|^2} \tilde{\Gamma}_{nn}^{\alpha\beta}(z) \frac{p_n^\beta}{|p_n|^2}, \quad |p_n|^2 = \sum_\alpha (p_n^\alpha)^2. \quad (13)$$

Using this relationship the conditionally-averaged LDOS can be expressed as

$$\tilde{\rho}_n(\omega) = -\frac{1}{\pi} \text{Im} \sum_{\alpha,\beta} \frac{p_n^\alpha}{|p_n|^2} \tilde{\Gamma}_{nn}^{\alpha\beta}(\omega) \frac{p_n^\beta}{|p_n|^2}, \quad (14)$$

while the total DOS is found in terms of $\tilde{\Gamma}_{nn}^{\alpha\beta}(z)$ as a trivial single-site average

$$\bar{\rho}(\omega) = -\frac{1}{\pi} \text{Im} \sum_{\alpha,\beta} \left\langle \frac{p_n^\alpha}{|p_n|^2} \tilde{\Gamma}_{nn}^{\alpha\beta}(\omega) \frac{p_n^\beta}{|p_n|^2} \right\rangle. \quad (15)$$

Remarkably, the statistical averaging in the last formula can be performed immediately if the probability distribution of the transition dipoles is of the “purely orientational” form. The trace over vector indices of the conditionally-averaged GT depends only on the deterministic, in this case, absolute value of the n th-site dipole

moment $|p_n|$. The averaged GT and GF are related to each other as

$$\sum_\alpha \bar{\Gamma}_{nn}^{\alpha\alpha}(z) = |p_n|^2 \bar{G}_{nn}(z), \quad (16)$$

and consequently,

$$\bar{\rho}(\omega) = -\frac{1}{\pi |p_n|^2} \sum_\alpha \text{Im} \bar{\Gamma}_{nn}^{\alpha\alpha}(\omega). \quad (17)$$

The straightforward application of the averaging procedure to Eq. (10) gives the disorder-averaged linear polarizability in the form

$$\bar{\chi}^{\alpha\beta}(z) = -\mathcal{N} \sum_m [\bar{\Gamma}_{nm}^{\alpha\beta}(z) + \bar{\Gamma}_{nm}^{\alpha\beta*}(-z^*)]. \quad (18)$$

In order to reduce the double real-space summation we have used the translational invariance of $\bar{\Gamma}_{nm}^{\alpha\beta}(z)$ that allows to replace in both terms of Eq. (18) $\sum_{n,m} \bar{\Gamma}_{nm}^{\alpha\beta}(z)$ by $\mathcal{N} \sum_m \bar{\Gamma}_{nm}^{\alpha\beta}(z)$. The last sum here is already converging and does not depend on its upper limit \mathcal{N} . Equivalently,

$$\bar{\chi}^{\alpha\beta}(z) = -\mathcal{N} \left[\bar{\Gamma}_{k=0}^{\alpha\beta}(z) + \bar{\Gamma}_{k=0}^{\alpha\beta*}(-z^*) \right], \quad (19)$$

where the momentum-domain disorder-averaged GT is introduced according to

$$\bar{\Gamma}_{nm}^{\alpha\beta}(z) = \int_{-\pi}^{\pi} \frac{dk}{2\pi} e^{ik(n-m)} \bar{\Gamma}_k^{\alpha\beta}(z), \quad (20)$$

k being measured in units of the inverse lattice spacing. Noticeably, the above polarizability scales linearly with the number \mathcal{N} of molecules constituting the aggregate. Unlike the physics coming from the nontrivial dependence of $\bar{\Gamma}_{nm}^{\alpha\beta}(z)$ on the energy variable z and the intersite separation $|n - m|$ this elementary aspect is not related to the degree of exciton coherence. Nevertheless it guarantees fulfillment of an important part of the general sum rule according to which the polarizability is an extensive quantity proportional to the total number of polarizable objects.

C. Coherence length

In the literature dealing with the optics of molecular aggregates it is usually introduced the notion of the exciton coherence length^{11,12,15,17} to characterize the spatial extension of the exciton wave functions. The cited works, addressing the problem mainly with numerical methods, employ several definitions of this parameter to be extracted from the set of wave functions obtained with explicit diagonalization procedures. Even though the quantitative estimates provided within all approaches can be in reasonable agreement with each other, the physical arguments used are somewhat different. From the viewpoint of the present work a natural definition of the exciton coherence length can be given on the basis of Eq. (18).

In fact, entering it the disorder-averaged single-exciton GT contains all the information on the linear optical response of the excitonic system and depends nontrivially on the amplitude and phase coherence between the wave functions for different disorder realizations. These coherence properties partly reveal themselves in the DOS and absorption spectra which can be essentially different from those of the disorder-free system, but it is also the dependence of $\bar{\Gamma}_{nm}^{\alpha\beta}(z)$ on the intersite separation that gets strongly affected by the structural disorder within the chain. Excluding some peculiar cases,³³ each component of the disorder-averaged GT is characterized by an exponential behavior

$$\bar{\Gamma}_{nm}^{\alpha\beta}(z) \sim \exp(i\xi^{\alpha\beta}(z)|n - m|), \quad |n - m| \rightarrow \infty, \quad (21)$$

where $\xi^{\alpha\beta}(z)$ is a complex-valued wave number. Keeping in mind this asymptotics while performing the real-space summation in Eq. (18) one concludes that the dominant contribution to the disorder-averaged polarizability $\bar{\chi}^{\alpha\beta}(z)$ comes from the pairs of sites with $\text{Im } \xi^{\alpha\beta}(z)|n - m| \lesssim 1$. The parameter

$$N^{\alpha\beta}(z) = \frac{1}{\text{Im } \xi^{\alpha\beta}(z)}, \quad (22)$$

indicating how many molecules contribute to a given component of the linear polarizability, provides a natural definition of the exciton coherence length. Clearly, $N^{\alpha\beta}(z)$ is a straightforward generalization of the conventional quasiparticle phase coherence length, defined in terms of the large-intersite-separation asymptotics of the GF, to incorporate the vectorial nature of the excitonic polarization. The quantity (22) can be also thought of as the nonlocality range of the linear optical response function.

III. BEB-CPA SCHEME

A. Main procedure

As already mentioned, in order to find the statistical averages (11) and (12) we shall employ the single-site self-consistent approximation known as BEB CPA.²⁵ This theory is capable to address simultaneously both diagonal and off-diagonal disorder, provided the second enters the random Hamiltonian in a generalized multiplicative form. The last condition is intrinsically fulfilled in the excitonic problem under consideration because the coupling (2) is given by a bilinear combination of the random p_n^α with $\vartheta_{nm}^{\alpha\beta}$ being translationally-invariant deterministic matrix. The BEB extension of the scalar CPA¹⁹ is based on the so-called BEB transformation.²⁵ The latter represents a vector generalization of the multiplicative ansatz originally implemented by Shiba²⁴ to construct a single-site self-consistent theory for bond-disordered alloys with mean-geometric relationship between hopping integrals. Upon such transformation the

problem of finding the resolvent of a Hamiltonian with both diagonal and multiplicative off-diagonal disorder is equivalently reformulated for an operator which acts in a space with additional tensorial dimensions but contains only site-diagonal disorder. With application to Frenkel excitons the BEB transformation has been already realized in Sec. II B by considering instead of operators B_n^\dagger (B_n) the polarizations $P_n^{\alpha(+)}$ ($P_n^{\alpha(-)}$) equipped with vector indices. As a consequence the dynamical equation for the scalar GF,

$$G_{nm}(z) = g_n(z)\delta_{nm} + g_n(z) \sum_l J_{nl} G_{lm}(z), \quad (23)$$

is replaced with that for the GT,

$$\Gamma_{nm}(z) = \gamma_n(z)\delta_{nm} + \gamma_n(z) \sum_l \vartheta_{nl} \Gamma_{lm}(z). \quad (24)$$

[Here and below omitting the indices we assume the usual rules for multiplication and inversion of tensorial quantities.] Unlike the case of Eq. (23), the disorder enters Eq. (24) only in the site-diagonal form, namely, through the tensor

$$\gamma_n^{\alpha\beta}(z) = p_n^\alpha g_n(z) p_n^\beta \quad (25)$$

associated with the bare local GF

$$g_n(z) = \frac{1}{z - \epsilon_n}. \quad (26)$$

At the same time, because the algebraic structure of equation (24) remains similar to that of (23), the usual CPA self-consistency arguments can be employed to approximate the statistical averages defined in Eqs. (11) and (12). The BEB-CPA scheme²⁵ is accomplished via straightforward generalization of the scalar-CPA equations within the tensorial formalism as outlined below.

The disorder effect on the single-particle quantities is accounted in CPA by replacing the random local GTs $\gamma_n^{\alpha\beta}(z)$ with a deterministic site-independent coherent-potential GT $\gamma^{\alpha\beta}(z)$. The disorder-averaged GT in the momentum representation is found from Eq. (24) as

$$\bar{\Gamma}_k(z) = [1 - \gamma(z)\vartheta_k]^{-1} \gamma(z), \quad (27)$$

where

$$\vartheta_k^{\alpha\beta} = \frac{1}{N} \sum_{n,m} e^{-ik(n-m)} \vartheta_{nm}^{\alpha\beta} \quad (28)$$

is the momentum-space coupling kernel. In turn, the conditionally-averaged on-site GT $\bar{\Gamma}_{nn}^{\alpha\beta}(z)$ is approximated by assuming that the site, carrying its random parameters, is placed into the same coherent environment as the one of Eq. (27). Thus, finding this conditional average reduces to solving a single-impurity problem realized by Eq. (24) in which the bare GTs $\gamma_m^{\alpha\beta}(z)$ for $m \neq n$ are

replaced by $\gamma^{\alpha\beta}(z)$. A simple derivation^{20,25,26,27} leads to

$$\bar{\Gamma}_{nn}(z) = [1 - \gamma_n(z)\Sigma(z)]^{-1} \gamma_n(z), \quad (29)$$

where the site-diagonal self-energy $\Sigma^{\alpha\beta}(z)$ describes coupling of the selected molecule with the coherent-background molecules constituting the rest of the chain. Clearly, being a functional of only the coherent-potential GT $\gamma^{\alpha\beta}(z)$, this self-energy is the same as the one entering the complete disorder-average of the local GT

$$\bar{\Gamma}_{nn}(z) = [1 - \gamma(z)\Sigma(z)]^{-1} \gamma(z). \quad (30)$$

Provided both $\gamma^{\alpha\beta}(z)$ and $\bar{\Gamma}_{nn}^{\alpha\beta}(z)$ are represented by non-singular matrices one gets

$$\Sigma(z) = \gamma^{-1}(z) - \bar{\Gamma}_{nn}^{-1}(z), \quad (31)$$

where the local GT is found in terms of $\gamma^{\alpha\beta}(z)$ from Eq. (27) after the momentum-space integration:

$$\bar{\Gamma}_{nn}(z) = \int_{-\pi}^{\pi} \frac{dk}{2\pi} [1 - \gamma(z)\vartheta_k]^{-1} \gamma(z). \quad (32)$$

The unknown coherent-potential GT $\gamma^{\alpha\beta}(z)$ is to be determined in a self-consistent way. In spirit of the original CPA, one demands the single-site expectation of the conditionally-averaged GT to coincide with the completely-averaged local GT:

$$\bar{\Gamma}_{nn}^{\alpha\beta}(z) = \langle \tilde{\Gamma}_{nn}^{\alpha\beta}(z) \rangle. \quad (33)$$

The latter guarantees that the conditional and the complete average of the GT found above will provide identical estimates for the single-site quantities such as LDOS or the local (single-molecule) polarizability.

Summarizing, the BEB-CPA procedure amounts to solving equations which, including auxiliary definitions, are listed in formulas from (25) to (33). For nontrivial disorder models and realistic forms of the coupling $\vartheta_{nm}^{\alpha\beta}$ this can be done only with the use of numerical methods. An example of such numerical solution is given in Sec. V [see also Appendix A]. The analytic treatment of the low-disorder limit of the theory is presented in Sec. IV.

B. Analyticity and accuracy of BEB CPA

As clear from the general discussion of Sec. II B, the BEB CPA allows to find configurational averages of the exciton DOS and linear polarizability of a disordered molecular aggregate. It is natural to check the validity of such nonperturbative theory asking, in particular, how close are the estimates to the actual quantities and whether they meet certain fundamental physical requirements. This question can be partly answered by analyzing the structure of the BEB-CPA equations as done in a number of publications.^{20,25,26,27,28} For completeness,

let us outline the important facts concerning analyticity and accuracy of the BEB CPA.

Gonis and Garland²⁷ have proved that $\bar{\Gamma}_{nm}^{\alpha\beta}(z)$ found within BEB CPA possesses the same properties as a function of the complex energy z as would have the disorder-averaged GT calculated exactly. Namely, it is analytic in the whole plane excluding branch cuts on the semi-axis $\text{Im } z = 0$, $\text{Re } z > 0$, while the tensor

$$\bar{A}_k^{\alpha\beta}(z) = -\frac{1}{2\pi i} [\bar{\Gamma}_k^{\alpha\beta}(z) - \bar{\Gamma}_k^{\beta\alpha*}(z)], \quad (34)$$

that at $z = \omega + i0^+$ provides the exciton spectral density, is positively (negatively) defined at $\text{Im } z > 0$ ($\text{Im } z < 0$). As a consequence the disorder-averaged polarizability will preserve causality, while the DOS and absorption will be nonnegative.

The authors of Ref. 25 have studied the accuracy of the theory to reproduce the energy-domain moments of the spectral density, each given by a coefficient in the high-energy expansion of the GT:

$$\bar{\Gamma}_k^{\alpha\beta}(z) = \sum_{s=0}^{\infty} \frac{L_{k,s}^{\alpha\beta}}{z^{s+1}}, \quad L_{k,s}^{\alpha\beta} = \int_0^{+\infty} d\omega \omega^s \bar{A}_k^{\alpha\beta}(\omega). \quad (35)$$

It was shown that the BEB CPA provides correctly the first three moments of the spectral density,

$$\begin{aligned} L_{k,0} &= l_0, & L_{k,1} &= l_1 + l_0 \vartheta_k l_0, \\ L_{k,2} &= l_2 + l_1 \vartheta_k l_0 + l_0 \vartheta_k l_1 + l_0 \vartheta_k l_0 \vartheta_k l_0, \end{aligned} \quad (36)$$

where the corresponding moments entering the high-energy expansion of the local coherent-potential GT $\gamma^{\alpha\beta}(z)$ are given by

$$\begin{aligned} l_0^{\alpha\beta} &= \langle p_n^{\alpha} p_n^{\beta} \rangle, & l_1^{\alpha\beta} &= \langle p_n^{\alpha} \epsilon_n p_n^{\beta} \rangle, \\ l_2^{\alpha\beta} &= \langle p_n^{\alpha} \epsilon_n^2 p_n^{\beta} \rangle + \sum_{\gamma,\delta} [\langle p_n^{\alpha} p_n^{\gamma} p_n^{\delta} p_n^{\beta} \rangle - \langle p_n^{\alpha} p_n^{\gamma} \rangle \langle p_n^{\delta} p_n^{\beta} \rangle] \\ &\quad \times \int_{-\pi}^{\pi} \frac{dk}{2\pi} \sum_{\mu,\nu} \vartheta_k^{\gamma\mu} \langle p_n^{\mu} p_n^{\nu} \rangle \vartheta_k^{\nu\delta}. \end{aligned} \quad (37)$$

The fact that the number of these moments is high enough guarantees fulfillment of the sum rules for the DOS and polarizability, correctly accounting for redistribution of the total oscillator strength between components of the polarizability tensor in the presence of orientational disorder. It follows also that using BEB CPA one gets an exact value of the absorption linewidth, *provided* the latter is defined from the weighted second centered moment of the spectral density $[\eta^{\alpha\beta} \sim \sqrt{L_{k=0,2}^{\alpha\beta} L_{k=0,0}^{\alpha\beta} - (L_{k=0,1}^{\alpha\beta})^2} / L_{k=0,0}^{\alpha\beta}]$. This means that, even though there exists no unique way to define the width of an inhomogeneously-broadened absorption line, the BEB CPA still gives a reasonable estimate for this characteristics of the spectrum.

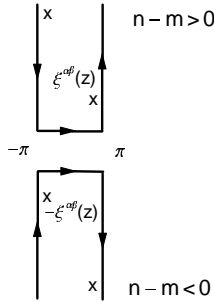


FIG. 1: Schematic picture of the integration contour in the complex momentum plane. Each couple of vertical lines with opposite orientations give zero contribution to the integral. The crosses mark poles of the momentum-space GT.

Let us also mention that the theory does not seem to violate the fundamental inequalities $|E - \epsilon_n| \leq \sum_m |J_{nm}|$ to be fulfilled for every eigenvalue E . These, in particular, impose the lower, $\min(\epsilon_n - \sum_m |J_{nm}|)$, and the upper, $\max(\epsilon_n + \sum_m |J_{nm}|)$, bounds of the spectral region, where minimum and maximum are taken over all disorder realizations. Even though no rigorous proof of this property is known for the case of BEB CPA, it was shown to hold in the numerical solution of the BEB-CPA equations for some random alloy models.²⁸ As will be demonstrated in Sec. V, these spectral bounds are not violated in the case of orientational disorder either.

Another important aspect of the theory is the behavior of the disorder-averaged GT in the complex momentum domain. Considering $\tilde{\Gamma}_k^{\alpha\beta}(z)$ for complex k provides additional understanding about the exciton coherence length. Since $\tilde{\Gamma}_k^{\alpha\beta}(z)$ remains the same as $\text{Re } k$ is shifted by integer of 2π , the integration contour in Eq. (20) can be modified as shown in Fig. 1. Provided the function is meromorphic (i.e., has only isolated poles) in k , the integration reduces to sum over poles in the upper (lower) half-plane for $n - m > 0$ ($n - m < 0$). [Due to the mirror symmetry of the problem each pole has a counterpart located symmetrically with respect to the origin $k = 0$.] To establish connection with the coherence length defined above it is sufficient to notice that only a single pair of poles will contribute to the asymptotics (21), namely, having minimal distance from the real axis $\text{Im } k = 0$. Applying these arguments to the disorder-averaged GT in the BEB-CPA form (27) one concludes that the complex wave numbers $\xi^{\alpha\beta}(z)$ of Eq. (21) are to be selected among the solutions k of the characteristic equation

$$\det [1 - \gamma(z)\vartheta_k] = 0. \quad (38)$$

Here we assumed that the Fourier-transformed kernel $\vartheta_k^{\alpha\beta}$ is analytic in k to provide meromorphic $\tilde{\Gamma}_k^{\alpha\beta}(z)$. This assumption is valid, for instance, if the coupling extends only over a finite number of sites. However, the last equation may not lead to a correct coherence length for a more general nonanalytic coupling.

IV. LOW-DISORDER LIMIT

For a disorder-free chain the GT obtained from the BEB CPA coincides with the one known exactly. In order to establish the relation of our approach with the existing scaling theories of disordered one-dimensional excitons⁵ let us solve the BEB-CPA equations in the limit of weak disorder. A similar calculation for the bond-disordered binary alloy has been already done in Ref. 28. However, due to the rather involved structure of BEB CPA the general treatment of the low-disorder regime is still missing. For the sake of simplicity we shall also relax generality imposing certain symmetries under which the theory is formulated in terms of diagonal tensors.

A. General

To proceed one needs first to specify the “low” disorder in terms of its probability distribution, entering the BEB CPA through the self-consistency equation (33). We do this imposing smallness of the centered moments of the probability density which characterize deviations of the on-site energies and transition dipoles from their average values $\epsilon = \langle \epsilon_n \rangle$, $p^\alpha = \langle p_n^\alpha \rangle$. The conditionally-averaged local GT in Eq. (33) can be represented as a power series in $\epsilon_n - \epsilon$ and $p_n^\alpha - p^\alpha$, so that its n th-site expectation can be written as

$$\langle \tilde{\Gamma}_{nn}^{\alpha\beta}(z) \rangle = \sum_\nu \langle \tilde{\Gamma}_{nn}^{\alpha\beta}(z) \rangle_\nu. \quad (39)$$

A ν th term in the last sum is proportional to the ν th-order centered moments of the probability density. The first three terms are given explicitly by

$$\begin{aligned} \langle \tilde{\Gamma}_{nn}(z) \rangle_0 &= \tilde{\Gamma}_{nn}(z) \Big|_{\epsilon_n = \epsilon, p_n^\alpha = p^\alpha}, \\ \langle \tilde{\Gamma}_{nn}(z) \rangle_1 &= 0, \\ \langle \tilde{\Gamma}_{nn}(z) \rangle_2 &= \frac{1}{2} \left[a_2 \frac{\partial^2 \tilde{\Gamma}_{nn}(z)}{\partial \epsilon_n^2} + \sum_\alpha b_2^\alpha \frac{\partial^2 \tilde{\Gamma}_{nn}(z)}{\partial \epsilon_n \partial p_n^\alpha} \right. \\ &\quad \left. + \sum_{\alpha, \beta} c_2^{\alpha\beta} \frac{\partial^2 \tilde{\Gamma}_{nn}(z)}{\partial p_n^\alpha \partial p_n^\beta} \right] \Big|_{\epsilon_n = \epsilon, p_n^\alpha = p^\alpha}, \end{aligned} \quad (40)$$

where in the last equation

$$\begin{aligned} a_2 &= \langle (\epsilon_n - \epsilon)^2 \rangle, & b_2^\alpha &= \langle (\epsilon_n - \epsilon)(p_n^\alpha - p^\alpha) \rangle, \\ c_2^{\alpha\beta} &= \langle (p_n^\alpha - p^\alpha)(p_n^\beta - p^\beta) \rangle \end{aligned} \quad (41)$$

are the second-order centered moments. The terms not included in Eq. (40) will be neglected following our assumption about weakness of disorder. Later it will be demonstrated that the information contained in the third- and higher-order centered moments is indeed not preserved in the low-disorder limit of BEB CPA.

We shall additionally impose some simplifying restrictions on the form of disorder and intermolecular coupling to be considered below. Namely, let the system to be such that (i) in some (orthogonal) basis of the three-dimensional vector space the coupling $\vartheta_{nm}^{\alpha\beta}$ is diagonal in the upper indices for all pairs of molecules, and (ii) the disorder probability density is symmetric under reflections of two basis vectors. We shall label tensorial components corresponding to either these two basis vectors by symbols “ \perp_1 ”, “ \perp_2 ”, and those of the remaining (third) vector by “ \parallel ”. The coupling energies J_{nm} and, hence, the scalar GF $G_{nm}(z)$ remain invariant, while every off-diagonal tensorial component of the GT $\Gamma_{nm}^{\alpha\beta}(z)$ changes its sign under one of the above reflections [because from $\alpha \neq \beta$ it follows that either α or β is different from \parallel]. Therefore, configurational averaging with a symmetric probability distribution will result to a diagonal $\tilde{\Gamma}_{nn}^{\alpha\beta}(z)$.

Regarding the BEB-CPA theory, from Eqs. (27) and (30) it follows consecutively that both the coherent-potential GT $\gamma^{\alpha\beta}(z)$ and the self-energy $\Sigma^{\alpha\beta}(z)$ reduce to the diagonal form. As concerns the low-disorder limit to be studied here, with our symmetry requirements the average dipole moment p^α is directed strictly along the \parallel -axis, the vectorial parameter b_2^α defined in Eq. (41) has nonzero component only along the same axis, while the tensor $c_2^{\alpha\beta}$ is diagonal. Using the explicit dependence of the conditionally-averaged GT on the n th site random parameters [see Eqs. (25), (26) and (29)] the nontrivial (diagonal) components of the tensors (40) can be found as

$$\langle \tilde{\Gamma}_{nn}^{\parallel}(z) \rangle_0 = \frac{|p|^2}{z - \epsilon - \Sigma^{\parallel}(z)|p|^2}, \quad \langle \tilde{\Gamma}_{nn}^{\perp_i}(z) \rangle_0 = 0, \quad (42)$$

$$\begin{aligned} \langle \tilde{\Gamma}_{nn}^{\parallel}(z) \rangle_2 &= \frac{a_2|p|^2}{[z - \epsilon - \Sigma^{\parallel}(z)|p|^2]^3} \\ &+ \frac{2b_2^{\parallel}|p|}{[z - \epsilon - \Sigma^{\parallel}(z)|p|^2]^2} \\ &+ \frac{c_2^{\parallel}(z - \epsilon)[z - \epsilon + 3\Sigma^{\parallel}(z)|p|^2]}{[z - \epsilon - \Sigma^{\parallel}(z)|p|^2]^3} \\ &+ \sum_{i=1,2} \frac{c_2^{\perp_i}\Sigma^{\perp_i}(z)|p|^2}{[z - \epsilon - \Sigma^{\parallel}(z)|p|^2]^2}, \quad (43) \\ \langle \tilde{\Gamma}_{nn}^{\perp_i}(z) \rangle_2 &= \frac{c_2^{\perp_i}}{z - \epsilon - \Sigma^{\parallel}(z)|p|^2}. \end{aligned}$$

Combined with the BEB-CPA self-consistency equation [Eq. (33)] these formulas provide the starting point for the analytical treatment of the low-disorder regime.

As seen from Eq. (43), the solution behaves quite differently in the two distinct spectral regions. Namely, if z is sufficiently far away from the singularities generated by denominator $z - \epsilon - \Sigma^{\parallel}(z)|p|^2$ one can look for the unknown $\gamma^{\alpha\beta}(z)$ in an approximate form, replacing in (43) the BEB CPA self-energy $\Sigma^{\alpha\beta}(z)$ with its

expression $\Sigma^{\alpha\beta(0)}(z)$ for the disorder-free system. The solution found in this way will be valid only for energies not very close to the band edges of the disorder-free system. Around these points one can no more neglect the disorder-induced corrections to the self-energy component $\Sigma^{\parallel(0)}(z)$ in Eq. (43). Nevertheless, the last situation is still addressable analytically because near the band edges an explicit asymptotic relation between $\tilde{\Gamma}_{nn}^{\alpha\beta}(z)$ and $\gamma^{\alpha\beta}(z)$ can be used.

B. Iterative solution

Away from the band edges of the disorder-free chain we can look for the coherent-potential GT in the iterative form

$$\gamma^{\alpha\beta}(z) = \gamma^{(0)\alpha\beta}(z) + \gamma^{(1)\alpha\beta}(z). \quad (44)$$

The first term with components

$$\gamma^{(0)\parallel}(z) = \frac{|p|^2}{z - \epsilon}, \quad \gamma^{(0)\perp_i}(z) = 0, \quad (45)$$

corresponds to the disorder-free system and $\gamma^{(1)\alpha\beta}(z)$ is a small correction to be determined. From equation (30) linearized in the parameters (41) one has

$$\gamma^{(1)\parallel}(z) = \frac{[z - \epsilon - \Sigma^{(0)\parallel}(z)|p|^2]^2}{(z - \epsilon)^2} \langle \tilde{\Gamma}_{nn}^{(0)\parallel}(z) \rangle_2, \quad (46)$$

$$\gamma^{(1)\perp_i}(z) = \langle \tilde{\Gamma}_{nn}^{(0)\perp_i}(z) \rangle_2,$$

where $\tilde{\Gamma}_{nn}^{(0)\alpha\beta}(z)$ denotes the local GT on a single impurity site in the disorder-free chain, related to the disorder-free self-energy $\Sigma^{(0)\alpha\beta}(z)$ by Eq. (29).

The computation of the disorder-free self-energy $\Sigma^{(0)\alpha\beta}(z)$ is not straightforward due to the fact that components $\gamma^{(0)\perp_i}(z)$ and $\tilde{\Gamma}_{nn}^{(0)\perp_i}(z)$ vanish leading to an undeterminate expression in Eq. (30). To overcome this difficulty one can employ the following arguments. Consider the disorder-free chain with a single impurity molecule placed on the n th site in such a way that its dipole moment p_n^α has no component along the \parallel -axis. Since in this case the transfer energy $J_{nm} = \sum_\alpha p_n^\alpha \vartheta_{nm}^{\alpha\beta} p_m^\beta$ vanishes, the n th site, decoupled from the rest chain, will be characterized by the local GT $\tilde{\Gamma}_{nn}^{(0)\alpha\beta}(z)$ equal to the bare quantity $p_n^\alpha g_n(z) p_n^\beta$. From Eq. (29), for any of such p_n^α , it follows that $\sum_\alpha p_n^\alpha \Sigma^{(0)\alpha\beta}(z) p_n^\beta = 0$. Therefore, being a diagonal tensor, the self-energy will have nonzero projection only on the \parallel -axis, orthogonal to the subspace of the considered p_n^α . Using Eq. (31) for the nontrivial component of the self-energy we end up with a simple expression

$$\Sigma^{(0)\parallel}(z) = \frac{1}{|p|^2} \left[z - \epsilon - \frac{1}{\tilde{G}_{nn}^{(0)}(z)} \right], \quad \Sigma^{(0)\perp_i}(z) = 0, \quad (47)$$

where

$$\bar{G}_{nn}^{(0)}(z) = \int_{-\pi}^{\pi} \frac{dk}{2\pi} \frac{1}{z - \epsilon - \vartheta_k^{\parallel} |p|^2} \quad (48)$$

denotes the on-site scalar GF of the disorder-free chain. The first of Eqs. (47) represents a natural relationship between the scalar self-energy $z - \epsilon - 1/\bar{G}_{nn}^{(0)}(z)$ and the main component of the tensorial self-energy in the absence of disorder.

Having derived the disorder-free self-energy we get the desired correction (46) to the coherent-potential GT in the form

$$\begin{aligned} \gamma^{(1)\parallel}(z) &= \frac{a_2 |p|^2 \bar{G}_{nn}^{(0)}(z)}{(z - \epsilon)^2} + \frac{2b_2^{\parallel} |p|}{(z - \epsilon)^2} \\ &+ c_2^{\parallel} \left[4\bar{G}_{nn}^{(0)}(z) - \frac{3}{z - \epsilon} \right], \end{aligned} \quad (49)$$

$$\gamma^{(1)\perp_i}(z) = c_2^{\perp_i} \bar{G}_{nn}^{(0)}(z).$$

The final expression for the GT $\bar{\Gamma}_k^{\alpha\beta}(z)$, valid in the low-disorder regime away from the band edges, is obtained by inserting the total $\gamma^{\alpha\beta}(z)$ of Eq. (44) into (27).

Let us comment on the analytical properties of the obtained solution. The correction (49) obeys the large- z asymptotics $\gamma^{(1)\alpha\beta}(z) \sim c_2^{\alpha\beta}/z$. Hence, the disorder-averaged GT behaves as $\bar{\Gamma}_k^{\alpha\beta}(z) \sim (p^\alpha p^\beta + c_2^{\alpha\beta})/z$. Using definition (41) for $c_2^{\alpha\beta}$ it is easy to see that the coefficient $p^\alpha p^\beta + c_2^{\alpha\beta}$ coincides with that of the first term ($L_{k,0}^{\alpha\beta} = \langle p_n^\alpha p_n^\beta \rangle$) in the general high-energy expansion (35). That is, even though for the zero-order solution the asymptotics $\bar{\Gamma}_k^{(0)\alpha\beta}(z) \sim p^\alpha p^\beta/z$ is not accurate, the correct form is restored as the first-order iterative correction is taken into account. Furthermore, the next two coefficients ($L_{k,1}^{\alpha\beta}$, $L_{k,2}^{\alpha\beta}$) are also reproduced in the found solution provided one neglects the third- and the higher-order centered moments of the disorder distribution function in Eqs. (37). Nevertheless, the found GT can have in general spurious poles outside the real axis around the band-edge singularities of the disorder-free GF [Eq. (48)]. Such nonphysical behavior is related to the fact that around the band edge the second term in the expansion (44) is no more small as compared to the first. For the two components $\bar{\Gamma}_k^{\perp_i}(z)$ the portion of spectral weight taken up by the spurious poles vanishes upon decreasing the disorder strength $c_2^{\perp_i}$. This guarantees the correct reproduction of the optical absorption spectra for the corresponding polarizations, as well as the DOS away from the band edges. The same is true for the component $\bar{\Gamma}_k^{\parallel}(z)$ for a generic nonzero momentum k . On the other hand, the spectral density component $\bar{A}_k^{\parallel}(z)$ at momentum $k = 0$ is itself strongly concentrated near the energy

$$\zeta = \epsilon + \vartheta_{k=0}^{\parallel} |p|^2, \quad (50)$$

that usually represents an extremum of the bare exciton band. Hence, the iterative solution found in this section does not describe the most important part of the absorption profile for polarization directed along the average dipole moment.

C. Scaling solution

Let us now analyze the BEB-CPA equations near the lowest band edge of the disorder-free system. We shall use the standard (for J , but not H aggregates) assumption that this point corresponds to the center $k = 0$ of the Brilloiun zone, thus coinciding with the energy ζ defined in (50). Around $z = \zeta$ it is convenient to represent the \parallel -component of the coherent-potential GT as

$$\gamma^{\parallel}(z) = \frac{|p|^2}{z - \epsilon - \sigma(z)}. \quad (51)$$

Assuming the absolute value of the new unknown function $\sigma(z)$ to be small compared to the total width of the exciton band one can keep only a few significant terms in the expansion of the coupling kernel ϑ_k^{\parallel} around $k = 0$ while performing the momentum integration in Eq. (32). Provided the constant

$$J = \left. \frac{d^2 \vartheta_k^{\parallel}}{dk^2} \right|_{k=0} |p|^2 \quad (52)$$

has a finite (positive) value, that is the case if the real-space coupling $\vartheta_{nm}^{\parallel}$ decays faster than $|n - m|^{-3}$ at large intermolecular separation, we can use the effective mass approximation for the disorder-free exciton dispersion

$$\vartheta_k^{\parallel} |p|^2 \approx \vartheta_{k=0}^{\parallel} |p|^2 + \frac{J}{2} k^2. \quad (53)$$

This leads to the asymptotic expression for the corresponding component of the local GT valid around the band edge:

$$\bar{\Gamma}_{nn}^{\parallel}(z) = \frac{|p|^2}{\sqrt{2J} \sqrt{\zeta - z + \sigma(z)}}. \quad (54)$$

Furthermore, in accordance with Eq. (31), the respective self-energy can be represented as

$$\Sigma^{\parallel}(z) = \frac{1}{|p|^2} \left[z - \epsilon - \sigma(z) - \sqrt{2J} \sqrt{\zeta - z + \sigma(z)} \right]. \quad (55)$$

Concerning the two components $\bar{\Gamma}_{nn}^{\perp_i}(z)$, even though they share the singularity present in the above $\bar{\Gamma}_{nn}^{\parallel}(z)$, one can demonstrate that it is still possible to use the simple relationship $\bar{\Gamma}_{nn}^{\perp_i}(z) = \gamma^{\perp_i}(z)$, or equivalently to set $\Sigma^{\perp_i}(z) = 0$.

Writing the CPA self-consistency equation one can retain only the most singular terms of Eq. (43) near

the band edge $z \approx \zeta$ where for vanishing disorder also $\sigma(z) \approx 0$. The equation for $\gamma^{\perp i}(z)$ reads simply

$$\gamma^{\perp i}(z) = \frac{c_2^{\perp i}}{\sigma(z) + \sqrt{2J} \sqrt{\zeta - z + \sigma(z)}}. \quad (56)$$

As for the component $\gamma^{\parallel}(z)$, the only essential are the first and the third terms in the right-hand side of Eq. (43). By straightforward algebra we arrive at the self-consistency condition

$$\frac{\Delta^2 \sqrt{2J} \sqrt{\zeta - z + \sigma(z)}}{[\sigma(z) + \sqrt{2J} \sqrt{\zeta - z + \sigma(z)}]^2} = \sigma(z), \quad (57)$$

that represents an equation to be solved for $\sigma(z)$. In this formula we have used the shorthand notation

$$\Delta = \sqrt{a_2 + 4c_2^{\parallel}(\vartheta_{k=0}^{\parallel})^2 |p|^2} \quad (58)$$

for a combination which can be thought of as an effective disorder strength parameter governing the low-disorder limit of BEB CPA near the band edge.

The algebraic structure of equation (57) is still too complicated to obtain its solution in a closed form. At the same time the scaling of $\sigma(z)$ with the disorder strength Δ can be found easily. Namely, in the interval $|z - \zeta| \lesssim J(\Delta/J)^{4/3}$ the solution (both real and imaginary part) behaves as

$$\sigma(z) \sim J \left(\frac{\Delta}{J} \right)^{4/3}. \quad (59)$$

Employing this scaling relation one can find the low-disorder asymptotic expressions for the absorption linewidth and the exciton coherence length in the resonance region. Substituting (51) into Eq. (27) the main component of the disorder-averaged GT around the phase-space point $z \approx \zeta$, $k \approx 0$ can be written as

$$\bar{\Gamma}_k^{\parallel}(z) = \frac{|p|^2}{z - \zeta - \sigma(z) - Jk^2/2}. \quad (60)$$

The corresponding polarizability

$$\bar{\chi}^{\parallel}(z) = -\mathcal{N} \frac{|p|^2}{z - \zeta - \sigma(z)}, \quad (61)$$

obtained from the basic relation (19), is characterized by a resonant behavior near the band edge. The width of the resonance, estimated as $\eta^{\parallel} \sim -\text{Im} \sigma(\zeta)$, scales with the disorder strength Δ as

$$\eta^{\parallel} \sim J \left(\frac{\Delta}{J} \right)^{4/3}. \quad (62)$$

Furthermore, one can make use of the effective mass approximation (53) to get a scaling of the exciton coherence length in the spectral region around the absorption resonance. According to the arguments of Sec. III B

applied to expression (60), the complex wave number $k = \xi^{\parallel}(z)$ governing the asymptotic behavior of the disorder-averaged GT at large intermolecular separation is found from equation

$$z - \zeta - \sigma(z) - \frac{J}{2} k^2 = 0. \quad (63)$$

Taking $z \approx \zeta$ we end up with the following scaling of the coherence length in the resonance region:

$$N^{\parallel} \sim \left(\frac{\Delta}{J} \right)^{-2/3}. \quad (64)$$

It should be also mentioned that combining Eq. (62) with (64) leads to the scaling relation

$$\eta^{\parallel} \sim J(N^{\parallel})^{-2}, \quad (65)$$

which does not involve the disorder strength Δ . This dependence is universal in the sense that it follows only from the shape of the exciton dispersion in the disorder-free system in the vicinity of the band edge. Indeed, the scaling (65) can be established without rigorous computation of the spectral density but by simply noticing that η^{\parallel} and $1/N^{\parallel}$ can be considered, respectively, as uncertainties of the exciton energy and momentum brought about by the disorder scattering. The relation between these quantities imposed by the dispersion (53) is of the quadratic form (65).

It can be noticed that the terms of expansion (39) proportional to the higher-order centered moments of the disorder distribution will bring stronger singularities in the vicinities of the band edges compared to ones of the second-order centered moments. Nevertheless, the dominant contribution to the solution will come solely from the second-order moments. Let us illustrate this for the simple situation when only diagonal disorder is present. A derivation analogous to that leading to Eq. (59) shows that the centered moment a_{ν} of order $\nu > 2$ alone would produce the scaling $\sigma_{\nu}(z) \sim J(a_{\nu}/J^{\nu})^{2/(1+\nu)}$. If the probability to encounter a random energy ϵ_n falls off rapidly enough away from the mean value ϵ we have $a_{\nu} \sim a_2^{\nu/2}$. Thus, the contribution $\sigma_{\nu}(z) \sim J(a_2/J^2)^{\nu/(1+\nu)}$ will be always suppressed by that of the second-order moment $\sigma(z) \sim J(a_2/J^2)^{2/3}$ considered so far.

When applied to a molecular chain with only diagonal disorder the asymptotic expressions (62) and (64) coincide with those obtained in Ref. 5 using different scaling arguments. Furthermore, for the case of diagonal disorder the asymptotics (62) has been found in Ref. 22 by means of the scalar CPA. Our theory thus provides an extension of these results treating both the on-site energy disorder and the disorder in transition dipoles on an equal footing through the combined parameter Δ of Eq. (58). The fact that BEB CPA is able to reproduce the known scaling relations is not surprising because this self-consistent approximation becomes exact in the disorder-free limit.

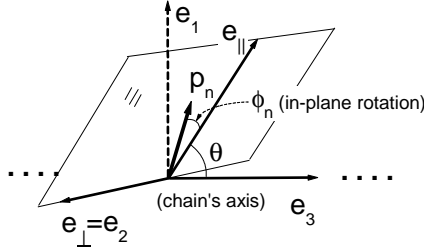


FIG. 2: The studied geometry of orientationally disordered molecular chain. The dipoles are distributed in the plane built on vectors e_{\parallel}^{α} , e_{\perp}^{α} and forming the angle θ with the chain's direction e_3^{α} .

V. ILLUSTRATIVE APPLICATIONS

A. Model and simplified parametrization

In this section we demonstrate how the general theory discussed so far can be applied to a specific model of disordered aggregate: a chain with purely orientational disorder in the transition dipoles. In addition to having constant absolute values the random dipoles will be assumed to lie in parallel planes forming an angle θ with the chain's direction [Fig. 2]. The random in-plane orientation angles ϕ_n will be modelled by a box probability with density $1/(2\Phi)$ in the interval $|\phi_n| < \Phi$ and zero outside. We shall consider the molecules to interact as dipoles in an isotropic background, so that the tensorial kernel $\vartheta_{nm}^{\alpha\beta}$ acquires the form

$$\begin{aligned} \vartheta_{nm}^{11} &= \vartheta_{nm}^{22} = V_{nm}, & \vartheta_{nm}^{33} &= -2V_{nm}, \\ \vartheta_{nm}^{12} &= \vartheta_{nm}^{13} = \vartheta_{nm}^{23} = 0. \end{aligned} \quad (66)$$

For the long-range (LR) dipole-dipole coupling one would have $V_{nm} = |n - m|^{-3}$. However, since in this case the momentum integral (32) can not be reduced to a closed analytic form, we shall restrict ourselves to the more easily treatable nearest-neighbor (NN) [$V_{nm} = \delta_{|n-m|,1}$] or next-nearest-neighbor (NNN) [$V_{nm} = \delta_{|n-m|,1} + \delta_{|n-m|,2}/8$] couplings. For concreteness we shall always assume that $\cos^2 \theta > 1/3$, so that the disorder-free chain ($\Phi = 0$) represents a J aggregate. The singular case $\cos^2 \theta = 1/3$ is considered separately in Appendix B. From now on the energy will be measured in the units of the NN interaction strength, and the dipoles will be chosen to have unit absolute values. We also shift the reference point of energy to the position of the bare molecular level.

Since the random dipoles are restricted in a single plane the theory can be conveniently reformulated in terms of tensors projected onto the corresponding two-dimensional subspace. We choose the new basis as

$$\begin{aligned} e_{\parallel}^1 &= \sin \theta, & e_{\parallel}^2 &= 0, & e_{\parallel}^3 &= \cos \theta, \\ e_{\perp}^1 &= 0, & e_{\perp}^2 &= 1, & e_{\perp}^3 &= 0, \end{aligned} \quad (67)$$

i.e., the first vector is parallel to dipoles of the disorder-free chain, the second is orthogonal to it and to the chain's axis. In terms of the projected components $p_{\parallel}^{\alpha} = \cos \phi_n$, $p_{\perp}^{\alpha} = \sin \phi_n$ the three-dimensional dipoles are given by

$$p_n^{\alpha} = e_{\parallel}^{\alpha} p_{\parallel}^{\alpha} + e_{\perp}^{\alpha} p_{\perp}^{\alpha}. \quad (68)$$

The advantages of this representation come from the fact that our disorder distribution density is invariant under the change of sign of p_n^{\perp} . Hence, since upon projection the coupling (66) remains diagonal,

$$\vartheta_{nm}^{\parallel} = (1 - 3 \cos^2 \theta) V_{nm}, \quad \vartheta_{nm}^{\perp} = V_{nm}, \quad (69)$$

the reduced BEB CPA will involve only diagonal tensors. As a result we end up with the affordable equations, whose explicit form for the case of NN and NNN coupling is given in Appendix A. Moreover, as the additional symmetry requirements formulated in Sec. IV are fulfilled, the low-disorder solution derived there can be employed. Since all components of a physically-measurable tensor can be straightforwardly reconstructed using Eq. (68) from the two diagonal components of the corresponding projected tensor, the last two will be presented every time to illustrate the outcome of the theory.

B. Numerical results

Due to their explicit form the equations of Appendix A can be efficiently solved using standard numerical methods. In order to test the accuracy of the theory we also performed exact diagonalization for an open chain of $N = 250$ molecules with either NN or LR coupling. The statistical error was reasonably small after averaging over 5000 disorder realizations with the energy domain divided into 400 output intervals.

The tensorial components of the coherent-potential GT are plotted against energy in Fig. 3. This figure can be used to illustrate analyticity of the theory and to predict certain features of the physical quantities to be presented below. Specifically, the functions $\text{Im } 1/\gamma^{\parallel}(\omega)$ and $\text{Im } 1/\gamma^{\perp}(\omega)$ obey the correct sign that guarantees the positivity of DOS and optical absorption. From Eq. (27) it follows that the resonant denominators of the exciton spectral density components are given by $[\text{Re } 1/\gamma(\omega) - \vartheta_k]^2 + [\text{Im } 1/\gamma(\omega)]^2$, where polarization labels \parallel or \perp are assumed. Hence, provided $\text{Im } 1/\gamma(\omega) \ll 1$, the spectral density will be characterized by a sharp resonance located around the frequency ω to be found from $\text{Re } 1/\gamma(\omega) - \vartheta_k = 0$. The solution of this equation for either polarization and momentum k can be found graphically from Fig. 3(c,d) [where, in particular, the positions of ϑ_k^{\parallel} and ϑ_k^{\perp} at $k = 0$ are shown with horizontal lines]. Actually, the assumption on smallness of the imaginary part of the inverse coherent-potential GT is valid only in the case of component $\gamma^{\parallel}(\omega)$ and only for moderately weak disorder. As concerns $\gamma^{\perp}(\omega)$, the above condition is

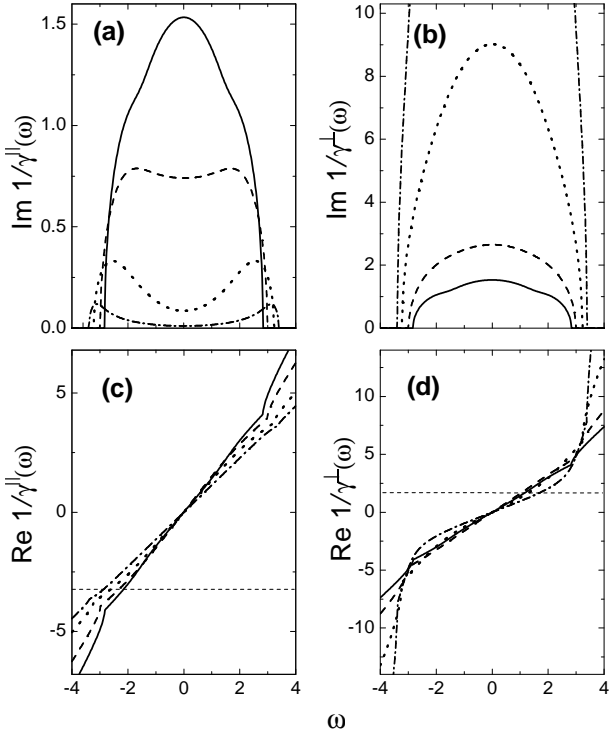


FIG. 3: The imaginary (a,b), and real (c,d) parts of the BEB-CPA self-energy for the case of NN coupling. Several values of the disorder parameter are used: $\Phi = 0.6$ (solid lines), $\Phi = 0.9$ (dashed lines), $\Phi = 1.3$ (dotted lines), $\Phi = 3.14$ (dash-dotted lines). $\theta = 0.26$ for all curves. The horizontal lines in panels (c) and (d) mark the diagonal elements of the NNN coupling matrix at momentum $k = 0$: $\vartheta_{k=0}^{\parallel} = -3.603$, $\vartheta_{k=0}^{\perp} = 2$.

never satisfied, so that one ends up with no well-defined quasiparticle peak in the corresponding component of the spectral density.

The profiles of the disorder-averaged exciton DOS are presented in Fig. 4. Except for the well-known band-center Dyson singularity³² in the case of NN coupling and a similar but nonsingular feature for the LR coupling³⁴ the numerical DOS is reproduced well within BEB CPA. As a confirmation of the analyticity of the theory no unphysical behavior of the DOS has been observed. The theory also captures properly the exact symmetry of the spectrum present in any tight-binding system without diagonal disorder and with only NN coupling. The asymmetric DOS in the case of LR interactions is satisfactorily approximated already by that of the NNN coupling. Furthermore, it can be observed that the upper and lower estimates of the spectrum region mentioned in Sec. III B are not violated in the presented solution. For instance, in the case of NN coupling the spectrum should not extend beyond the interval $|\omega| < 2 \max |J_{n,n+1}|$. The maximal absolute value of coupling accessible by varying parameters ϕ_n within the interval $|\phi_n| < \Phi$ is given differently in the distinct domains of the parametric space: if $\cos^2 \theta > 2/3$ it equals to $3 \cos^2 \theta - 1$, while in the op-

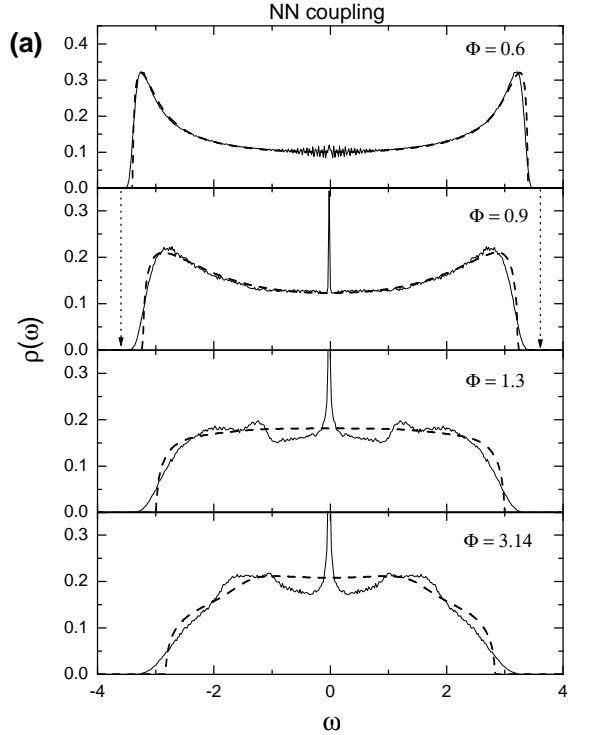


FIG. 4: The disorder-averaged exciton DOS for several values of disorder parameter Φ calculated with BEB CPA (dashed lines) or exact diagonalization (solid lines). (a) Case of NN coupling (both BEB CPA and exact diagonalization). (b) Case of NNN and DD coupling (BEB CPA) or LR coupling (exact diagonalization). $\theta = 0.26$ for all curves. The arrows mark the spectral bound estimates for the case of NN coupling and $\Phi = 0.9$, namely, $\omega = \pm 3.60$.

posite case it becomes $|1 - 3 \cos^2 \theta| \cos^2 \Phi + \sin^2 \Phi$ for $\Phi \leq \pi/2$, or 1 for $\Phi > \pi/2$.

The disorder-averaged absorption spectra (normalized by the number of molecules in the chain) along the two essential polarizations, e_{\parallel}^{α} and e_{\perp}^{α} , are presented in Fig. 5. The component $\text{Im } \bar{\chi}^{\parallel}(\omega)$, corresponding to the direction of preferable orientation of the dipoles, demonstrates behavior typical for disordered J aggregates: a sharp resonance acquiring inhomogeneous width upon increasing disorder is located near the bottom of the excitonic band. As for the polarization orthogonal to the preferred orien-

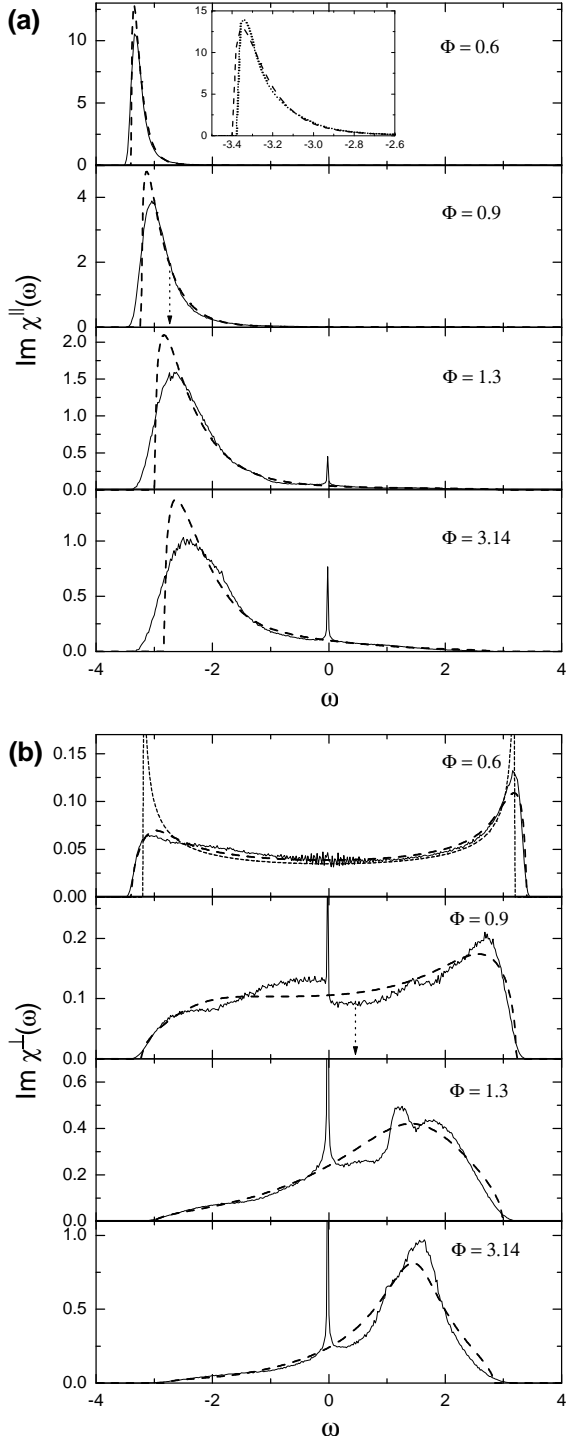


FIG. 5: The excitonic absorption spectra for NN coupling and several values of disorder parameter Φ calculated with BEB CPA (dashed lines) or exact diagonalization (solid lines). $\theta = 0.26$ for all curves. The arrows mark estimates of the spectral center for $\Phi = 0.9$: $\Omega^{\parallel} = -2.77$, $\Omega^{\perp} = 0.46$. For $\Phi = 0.6$ the absorption spectra resulting from the low-disorder limit of BEB CPA are presented (dotted lines).

tation of the dipoles, the absorption component $\text{Im } \bar{\chi}^{\perp}(\omega)$ is generated solely by orientational disorder. In contrast to the previous case no narrow resonance is observed, but rather a broad spectrum shifted to energies higher with respect to the bare molecular level. The positions of the absorption maxima can be roughly estimated from the zero and first moments of the spectral density as $\Omega^{\parallel} \sim L_{k=0,1}^{\parallel}/L_{k=0,0}^{\parallel}$, $\Omega^{\perp} \sim L_{k=0,1}^{\perp}/L_{k=0,0}^{\perp}$. Using Eqs. (36) for these parameters in the simplest case of NN coupling we end up with $\Omega^{\parallel} = (1 - 3 \cos^2 \theta)[1 + \sin 2\Phi/(2\Phi)]$, $\Omega^{\perp} = 1 - \sin 2\Phi/(2\Phi)$. These expressions one more time confirm that the centers of the absorption spectra are located at essentially different energies for the two polarizations.

To provide additional understanding of the features observed in the absorption spectra, the complete BEB-CPA spectral density is plotted in Fig. 6(a,b). For the considered disorder parameter ($\Phi = 0.9$) the component $\bar{A}_k^{\parallel}(\omega)$ is characterized by a well-pronounced quasiparticle structure with most of the spectral weight located around the disorder-free exciton branch $\omega = \vartheta_k^{\parallel}$. As for the part $\bar{A}_k^{\perp}(\omega)$, similarly to the already considered case of momentum $k = 0$ (the only directly accessible in the linear optics), the function has no resonant behavior in all the phase space. The spectral density transformed to the real-space representation is shown in Fig. 6(c,d). The component $\bar{A}_{nm}^{\parallel}(\omega)$ is essentially nonzero in the interval $|n - m| \lesssim 100$, and for fixed exciton energy has oscillatory behavior as a function of intermolecular distance $n - m$. Starting from zero near the bottom of the band the number of nodes monotonically increases as one moves towards the upper band edge. Since absorption is obtained from the real-space spectral density after the summation (18), the absence of oscillations explains the strong absorbance for the \parallel -polarization near the band bottom. As concerns polarization orthogonal to the preferred orientation of the transition dipoles, the function $\bar{A}_{nm}^{\perp}(\omega)$ is confined on a few ($|n - m| \lesssim 1 \div 2$) sites. This implies the absence of the coherent optical response of the molecules resulting to a weak and very broad absorption for this polarization direction.

Figure 7 illustrates variation of the exciton coherence length across the spectrum. The BEB-CPA coherence length has been found extracting the parameters $\xi^{\alpha\beta}(z)$ of the large-intersite-separation asymptotics (21) from Eq. (38). Owing to the symmetry of the problem the latter splits into the two independent equations $1 - \gamma^{\parallel}(z)\vartheta_k^{\parallel} = 0$, $1 - \gamma^{\perp}(z)\vartheta_k^{\perp} = 0$. Consequently, each of the two components $\bar{\Gamma}_{nm}^{\parallel}(z)$ and $\bar{\Gamma}_{nm}^{\perp}(z)$ is characterized by its own coherence length, to be denoted respectively as $N^{\parallel}(\omega)$ and $N^{\perp}(\omega)$. From the results presented in Fig. 7 it follows that $N^{\parallel}(\omega)$ strongly depends on energy, having maximum around the band center and decreasing as ω approaches the edges, whereas $N^{\perp}(\omega)$ is almost constant across the spectrum. Beyond the spectral region the parameters $\xi^{\alpha\beta}(\omega)$ are imaginary, and hence, the coherence length is finite, even in the uniform chain. Remarkably,

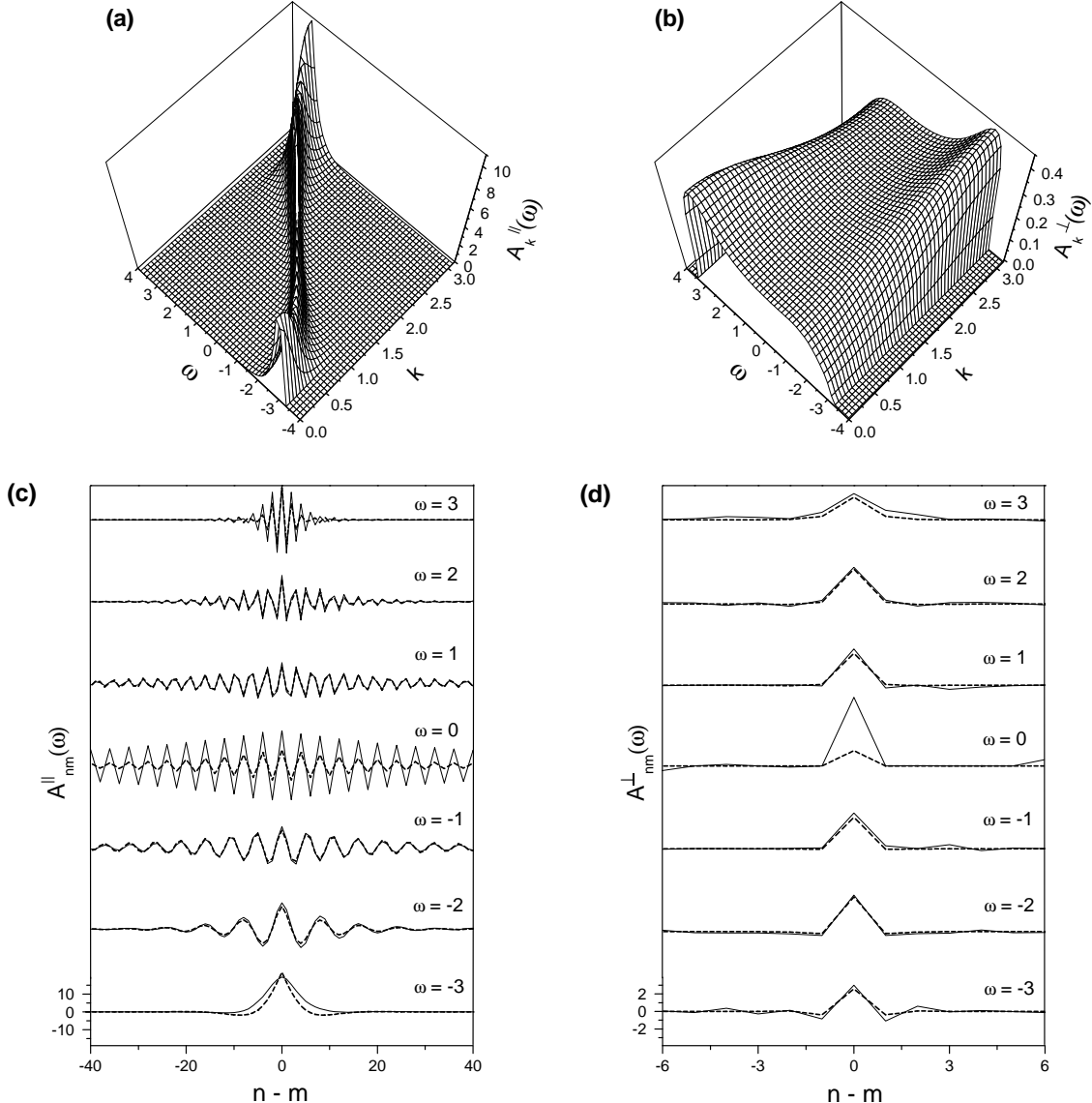


FIG. 6: (a,b) The tensorial components of the BEB-CPA exciton spectral density for the case of NN coupling. Only positive momenta k are shown. (c,d) The disorder-averaged spectral density in the real-space representation for a few fixed energies ω . The BEB-CPA results (dashed lines) are confronted with ones of the exact diagonalization (solid lines). The parameters are $\Phi = 0.9$, $\theta = 0.26$. [The strong discrepancy at $\omega = 0$ is the effect of the Dyson singularity not reproduced by the BEB CPA.]

upon variation of the parameter Φ the two lengths $N^{||}(\omega)$ and $N^{\perp}(\omega)$ evolve differently: the first decreases while the second grows with disorder. Regarding the exact diagonalization approach, the coherence length can be extracted directly from envelope of the disorder-averaged real-space spectral density in accordance with Eq. (21). Unlike the case of DOS and absorption, much larger statistical error is present owing to the fact that the quantity to be averaged (i.e., a tensorial component of the spectral density) depends on both energy and the real-space variables. Here one should keep small the width of the energy integration interval [$\delta\omega \approx 1/400$ of the total bandwidth in our simulations] to ensure that the additional decoherence due to interference of waves separated by

energies smaller than $\delta\omega$ does not exceed the disorder-induced effect. If $v(\omega)$ is the excitation group velocity the last condition can be expressed as $v(\omega)/\delta\omega \gg N^{||}(\omega)$. This inequality is not easy to fulfill around the band center [$N^{||}(\omega)$ is large] and around the band edges [$v(\omega)$ is small]. Apart from mentioned the numerical procedure suffers from the finite-size quantization taking place as the coherence length approaches the total length of the chain.

For the model under consideration we have also verified the accuracy of the low-disorder analytic solutions found in Sec. IV. Since no diagonal disorder is present the centered moments a_2 and b_2^{α} of the distribution vanish, and the only parameters which control the strength

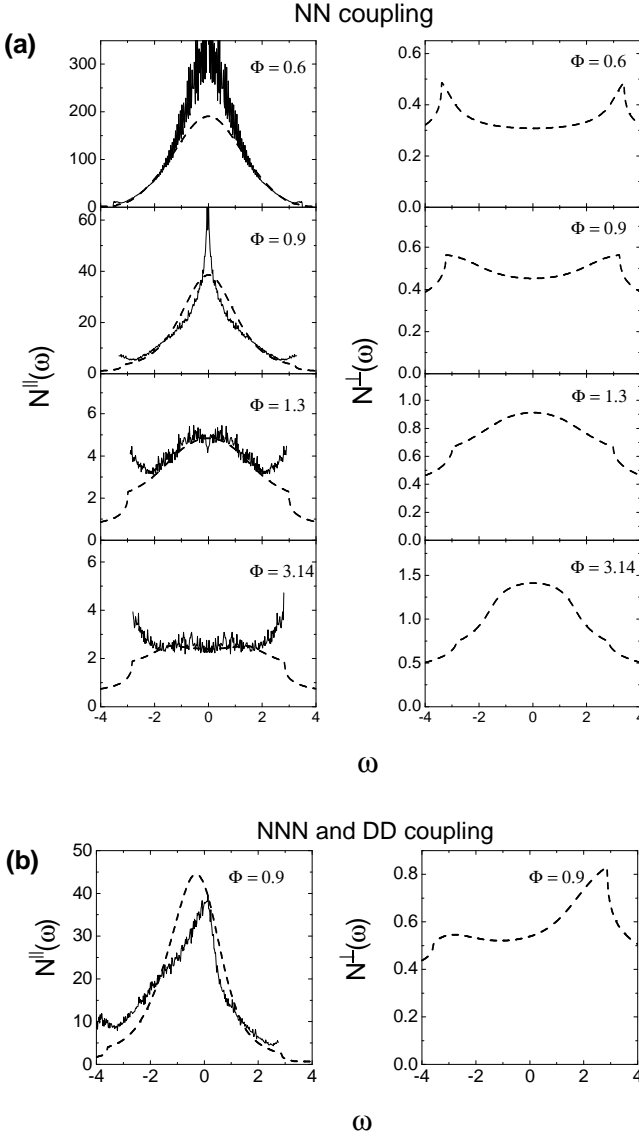


FIG. 7: Energy dependence of the exciton coherence length for several values of the disorder parameter Φ . The BEB-CPA results are presented in the case of both N^{\parallel} and N^{\perp} (dashed lines) and ones of the exact diagonalization (solid lines) only for N^{\parallel} . $\theta = 0.26$ for all curves.

of disorder are $c_2^{\parallel} \approx \Phi^4/45$ and $c_2^{\perp} \approx \Phi^2/3$. To evaluate these constants we have used Eq. (41) and retained only the leading terms in the limit of small Φ . In the magnitude of the averaged dipole moment one has to keep also the next-to-the-leading term, that results to the estimate $|p| \approx 1 - \Phi^2/6$. In Fig. 5 (panels with $\Phi = 0.6$) the analytic low-disorder absorption spectra are confronted with those calculated via direct solution of the BEB-CPA equations and by exact diagonalization. For polarization perpendicular to the preferred orientation of dipoles the spectral weight of the band-edge singularities (located at $\pm\zeta = \pm 2(1-3\cos^2\theta)$ for NN coupling) is negligible compared to the integrated spectral weight. To approximate such wide-bandwidth absorbance one can

use the iterative solution derived in Sec. IV B which results to expression $\text{Im } \bar{\chi}^{\perp}(\omega) \approx \mathcal{N} c_2^{\perp} / \sqrt{\zeta^2 - \omega^2}$. In contrast, the component $\text{Im } \bar{\chi}^{\parallel}(\omega)$, with most of the oscillator strength concentrated around the lower band edge, should be calculated using the approach of Sec. IV C. In particular, taking into account that the disorder parameter (58) is given by $\Delta \sim \Phi^2$, the scalings (62) and (64) read $\eta^{\parallel} \sim \Phi^{8/3}$, $N^{\parallel} \sim \Phi^{-4/3}$, respectively. The linewidth η^{\parallel} and the exciton coherence length N^{\parallel} at the absorption maximum extracted from the numerical solution of the BEB-CPA equations are plotted against Φ in Fig. 8(a,b). The presented profiles confirm the fulfillment of the derived scaling laws. Moreover, as illustrates Fig. 8(c), the universal scaling (65) is observed in the whole range of η^{\parallel} and N^{\parallel} accessible by varying Φ from 0 to π , even though the two above dependencies hold only for Φ sufficiently close to zero.

C. Experimental relevance

In a typical experiment one deals not with a single molecular chain but rather with a macroscopic ensemble of such objects. The treatment reported here is applicable only if the coupling between molecules of distinct aggregates is weaker than the disorder-induced broadening in a single chain. The broadening mechanisms not related to the considered types of disorder can be accounted for via a phenomenological on-site dephasing rate η , e.g., due to exciton-phonon scattering. The results of the BEB-CPA theory can be straightforwardly extended to include this case by adding imaginary contribution $i\eta$ to the complex energy variable z in all relevant functions.

In most of the samples accessible in experiment, such as frozen solutions containing molecular aggregates, because of the randomness in the chain's orientations one is not able to measure the individual spatial components of the microscopic (single-chain) polarizability tensor. Nevertheless, the available types of surface-deposited films³⁵ with strictly in-plane alignment or recently synthesized bulk materials with smectic-like³⁶ alignment of aggregates still allow for independent observation of certain spatial components of the single-chain polarizability. With a polarization-resolved spectroscopic study of such systems¹⁸ one can probe the orientational disorder within a single aggregate. In particular, a material obtained by stacking the chains described in Fig. 2 preserving perfectly parallel alignment of the axes and planes represents a biaxial medium. The optical axes are given by the directions e_{\parallel}^{α} , e_{\perp}^{α} , with the corresponding polarizabilities proportional to $\bar{\chi}^{\parallel}(\omega)$ and $\bar{\chi}^{\perp}(\omega)$, and the one orthogonal to them, along which the optical response vanishes.

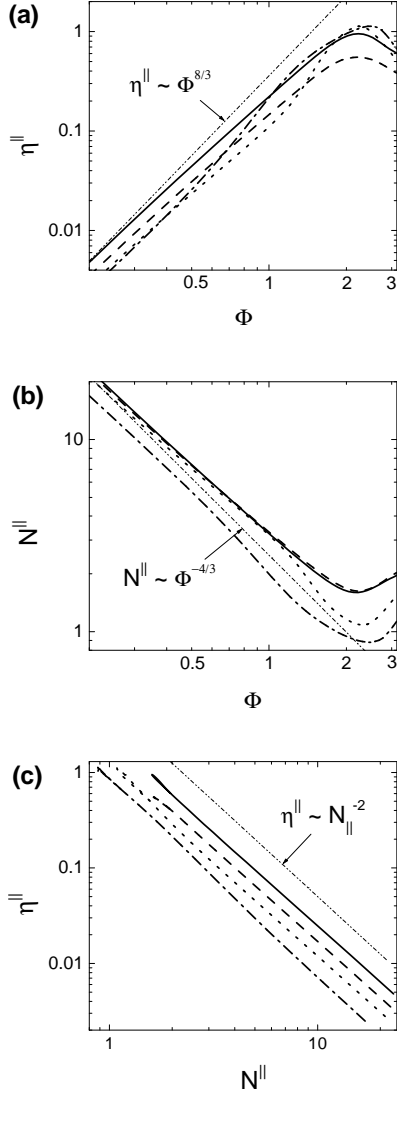


FIG. 8: Dependencies of the absorption linewidth (a) and the exciton coherence length at the resonance (b) on the disorder parameter Φ . (c) The same data is plotted in the coordinates “absorption linewidth — coherence length”. The parameter θ is 0.26 (solid line), 0.52 (dashed line), 0.65 (dotted line), 0.78 (dash-dotted line).

VI. CONCLUSIONS

In summary, using BEB CPA we have investigated the linear optical properties of a disordered molecular aggregate with random single-molecule excitation energies and transition dipoles. The advantages of the used self-consistent approximation are its analyticity, exactness in the low-disorder limit and the capability to provide not only the DOS and absorption spectra but also the coherence length. To the best of our knowledge, the last quantity has never been addressed in excitonic systems with the coherent-potential approximation. Whereas the DOS is on-site characteristics while the absorption spectrum is

related to the spectral density at momentum $k = 0$, the calculation of coherence length requires knowledge of the spectral density at a generic k . That is, the last quantity carries essentially new information on the single-particle properties of the system with respect to that contained in the first two.

The interesting feature of the considered problem is the tensorial structure of equations brought about by orientational disorder in the transition dipoles. Such type of disorder leads to redistribution of absorbance between different polarization components with quite distinct behavior of the corresponding coherence lengths.

Acknowledgments

We thank Professor F. Bassani for helpful discussions and encouragement and Dr D.M. Basko for suggestions on improving the manuscript. Financial support from U.V.O.-R.O.S.T.E. UNESCO, the European Union RTN-HYTEC and MIUR (PRIN-2001 “Advanced hybrid heterostructures”) is gratefully acknowledged.

APPENDIX A: BEB-CPA EQUATIONS FOR ORIENTATIONAL DISORDER WITH NN AND NNN COUPLING

In the case of box probability distribution the configurational averaging in the self-consistency equation (33) can be performed analytically leading to

$$(\Sigma^{\parallel} - \Sigma^{\perp})\bar{\Gamma}_{nn}^{\parallel} = q\sqrt{\frac{z - \Sigma^{\perp}}{z - \Sigma^{\parallel}}} - 1, \quad (A1a)$$

$$(\Sigma^{\perp} - \Sigma^{\parallel})\bar{\Gamma}_{nn}^{\perp} = q\sqrt{\frac{z - \Sigma^{\parallel}}{z - \Sigma^{\perp}}} - 1, \quad (A1b)$$

where function $q(z)$ is to be found from

$$\tan(q\Phi) = \sqrt{\frac{z - \Sigma^{\perp}}{z - \Sigma^{\parallel}}} \tan \Phi. \quad (A2)$$

From Eq. (31) the projected components of the self-energy can be expressed as

$$\Sigma^{\parallel} = \frac{1}{\gamma^{\parallel}} - \frac{1}{\bar{\Gamma}_{nn}^{\parallel}}, \quad \Sigma^{\perp} = \frac{1}{\gamma^{\perp}} - \frac{1}{\bar{\Gamma}_{nn}^{\perp}}. \quad (A3)$$

Performing momentum integration in Eq. (32) one relates the nontrivial components of the disorder-averaged on-site GT to the coherent-potential GT as

$$\bar{\Gamma}_{nn}^{\parallel} = \gamma^{\parallel} f((1 - 3 \cos^2 \theta) \gamma^{\parallel}), \quad \bar{\Gamma}_{nn}^{\perp} = \gamma^{\perp} f(\gamma^{\perp}). \quad (A4)$$

The function $f(x)$ entering these formulas is given by

$$\frac{1}{\sqrt{1 - 4x^2}},$$

and

$$\frac{2}{\sqrt{4+9x}} \left\{ \left[\left(\sqrt{8x} + \sqrt{4+9x} \right)^2 - 2x \right]^{-1/2} + \left[\left(\sqrt{8x} - \sqrt{4+9x} \right)^2 - 2x \right]^{-1/2} \right\},$$

for the cases of NN and NNN coupling, respectively.

For every disorder parameter Φ and tilt θ the equation presented in this Appendix can be solved numerically for $\gamma^{\parallel}(z)$ and $\gamma^{\perp}(z)$. The example of such solution is shown in Fig. 3.

APPENDIX B: FLAT-BAND SINGULAR SPECTRA

In this appendix we study the single-particle properties of the system described in Sec. V A when the angle θ formed by the plane of the transition dipoles with the chain's direction is such that $\cos^2 \theta = 1/3$ (i.e., $\theta = 0.955\dots$). The disorder-free situation for this value of θ can be considered as an intermediate case between that of J and H aggregate, because the transfer energy (2) generated by the dipolar coupling (66) vanishes. Neglecting higher multipole contributions to the transfer energy as well as all other broadening mechanisms which go beyond the present model, let us concentrate on the effect of orientational disorder to produce a finite excitonic bandwidth. [Considering instead the diagonal disorder alone results to a trivial physics: the off-diagonal part of the Hamiltonian is always zero and the molecules remain uncoupled.] Our aim is to find using BEB CPA the asymptotic form of the GT around $z = 0$, where the DOS and certain components of polarizability tensor have a singularity. [Such singularity due to specific arrangement of coupling and disorder should not to be confused with the Dyson singularity³², not accessible within BEB CPA]. For simplicity we shall consider only the case of NN coupling.

From Eq. (A4) with $\cos^2 \theta = 1/3$ it follows that $\bar{\Gamma}_{nn}^{\parallel}(z) = \gamma^{\parallel}(z)$. According to Eqs. (A3) the corresponding component of the BEB-CPA self-energy is zero, $\bar{\Sigma}^{\parallel}(z) = 0$. On the other hand $\Sigma^{\perp}(z)$ is nonzero at any finite z . Taking this into account it is easy to conclude that the auxiliary function defined by formula (A2) behaves as $q(z) \rightarrow \pi/(2\Phi)$ upon $z \rightarrow 0$. Applying the same limit to Eqs. (A1b) we get

$$\bar{\Gamma}_{nn}^{\perp}(z) \sim -\frac{1}{\Sigma^{\perp}(z)} \sim -\frac{i}{2}, \quad (B1)$$

$$\gamma^{\perp}(z) \sim -\frac{i\Phi}{\pi} \sqrt{\frac{2i}{z}}. \quad (B2)$$

Combining formula (B1) with Eq. (A1a) we obtain the asymptotics of the remaining unknown functions at $z \rightarrow$

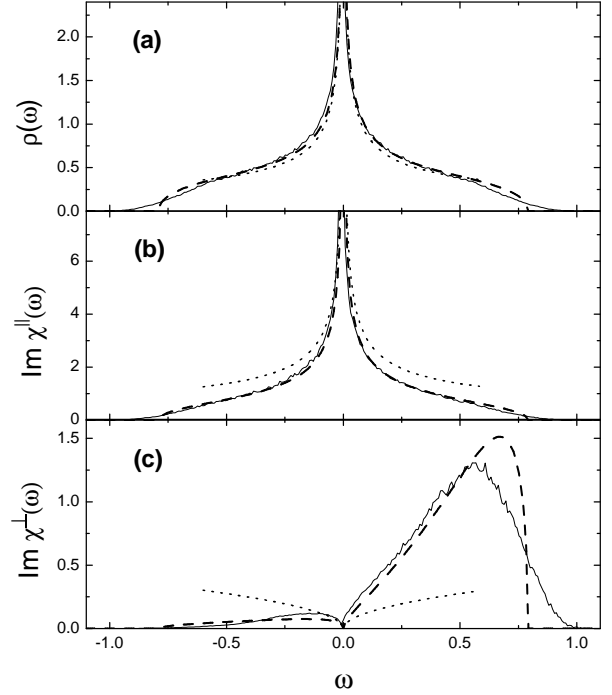


FIG. 9: (a) Exciton DOS and (b), (c) absorption spectra in the case $\cos^2 \theta = 1/3$. The BEB-CPA results (dashed lines) are confronted with ones of the exact diagonalization (solid lines) and the derived asymptotic expressions (dotted lines). The disorder parameter Φ is equal to 0.9 for all curves.

0:

$$\bar{\Gamma}_{nn}^{\parallel}(z) = \gamma^{\parallel}(z) \sim -\frac{i\pi}{4\Phi} \sqrt{\frac{2i}{z}}. \quad (B3)$$

It turns out that, irrespectively on the strength Φ of orientational disorder, the component $\bar{\Gamma}_{nn}^{\parallel}(z)$ of the disorder-averaged on-site GT is singular as $z \rightarrow 0$, i.e., at the energy of the bare molecular transition. Strictly speaking, upon introducing some degree of diagonal disorder or a finite inelastic dephasing rate η such singularity would be suppressed. Nevertheless, one can still apply the derived asymptotic formulas if the absolute value of z is much larger than η but smaller than the total bandwidth generated by orientational disorder.

The exciton DOS, related to the on-site GT found above by formula (17), shows an analogous singularity around $\omega = 0$:

$$\bar{\rho}(\omega) \sim \frac{1}{4\Phi} \frac{1}{\sqrt{|\omega|}}. \quad (B4)$$

As concerns the absorption spectra, for the two essential polarization directions these are characterized by completely distinct behavior:

$$\text{Im } \bar{\chi}^{\parallel}(\omega) \sim \frac{\mathcal{N}\pi}{4\Phi} \frac{1}{\sqrt{|\omega|}}, \quad \text{Im } \bar{\chi}^{\perp}(\omega) \sim \frac{\mathcal{N}\pi}{8\Phi} \sqrt{|\omega|}. \quad (B5)$$

The DOS and the absorption profiles calculated via numerical solution of the BEB-CPA equations and ones

of exact diagonalization are confronted with the derived asymptotic formulas in Fig. 9. All approaches agree well close to the band center. Noticeably, unlike the usual case $\cos^2 \theta \neq 1/3$, the absorption component $\text{Im } \bar{\chi}(\omega)$ is symmetric with respect to the central energy $\omega = 0$ (still only the NN coupling is assumed).

Regarding the exciton coherence length, since $\vartheta_k^{\parallel} = 0$ it follows that $N^{\parallel}(z) = 0$ for every z . In other words, for polarization along the preferred orientation of the dipoles the disorder-averaged spectral density depends on the intermolecular separation as $\text{Im } \bar{\Gamma}_{nm}^{\parallel}(z) \sim \delta_{nm}$, i.e., we encounter completely incoherent optical response of the molecules. For the orthogonal polarization in the vicinity of $z = 0$ we have

$$\xi^{\perp}(z) \sim \frac{\pi}{2} + \frac{i\pi}{2\Phi} \sqrt{\frac{z}{2i}}, \quad (\text{B6})$$

$$N^{\perp}(\omega) \sim \frac{4\Phi}{\pi} \frac{1}{\sqrt{|\omega|}}. \quad (\text{B7})$$

As a result the coherence length $N^{\perp}(\omega)$ is finite within the band but diverges at its center. In the vicinity of $\omega = 0$ the corresponding real-space spectral density behaves as $\text{Im } \bar{\Gamma}_{nm}^{\perp}(0) \sim \cos(\pi|n - m|/2)$, i.e., coincides with the center-of-the-band spectral density of a finite-bandwidth uniform chain.

* Electronic address: d.balagurov@sns.it

- ¹ E.E. Jolley, *Nature* **138**, 1009 (1936); G. Scheibe, *Angew. Chem.* **49**, 563 (1936)
- ² J. Knoester in *Organic Nanostructures: Science and Applications*, ed.s V.M. Agranovich and G.C. La Rocca (CXLIX course of "Enrico Fermi" School of Physics, SIF, 2002)
- ³ A.S. Davydov, *Theory of Molecular Excitons* (Plenum Press, New York, 1971)
- ⁴ E.W. Knapp, *Chem. Phys.* **85**, 73 (1984)
- ⁵ V.A. Malyshev, *Opt. Spectrosc.* **71**, 505 (1991)
- ⁶ H. Fidder, D.A. Wiersma, *Phys. Rev. Lett.* **66**, 1501 (1991)
- ⁷ J. Knoester, *Phys. Rev. A* **47**, 2083 (1993)
- ⁸ F. Domínguez-Adame, *Phys. Rev. B* **51**, 12801 (1995); F. Domínguez-Adame, B. Méndez, A. Sánchez, E. Maciá, *ibid.* **49**, 3839 (1994); F. Domínguez-Adame, *ibid.* **51**, 12801 (1995); V.A. Malyshev, A. Rodríguez, F. Domínguez-Adame, *ibid.* **60**, 14140 (1999)
- ⁹ V. Malyshev, P. Moreno, *Phys. Rev. B* **51**, 14587 (1995)
- ¹⁰ D.V. Makhov, V.V. Egorov, A.A. Bagatur'yants, M.V. Alfimov, *Chem. Phys. Lett.* **246**, 371 (1995)
- ¹¹ A.V. Malyshev, V.A. Malyshev, *Phys. Rev. B* **63**, 195111 (2001)
- ¹² H. Fidder, J. Knoester, D.A. Wiersma, *J. Chem. Phys.* **95**, 7880 (1991)
- ¹³ V.A. Malyshev, F. Domínguez-Adame, *Chem. Phys. Lett.* **313**, 255 (1999)
- ¹⁴ Th. Wagersreiter, H.F. Kauffmann, *Phys. Rev. B* **49**, 8655 (1994)
- ¹⁵ M. Shimizu, S. Suto, T. Goto, A. Watanabe, M. Matsuda, *Phys. Rev. B* **58**, 5032 (1998)
- ¹⁶ I. Avgin, D.L. Huber, *Phys. Rev. B* **60**, 7646 (1999)
- ¹⁷ D. Markovitsi, L.K. Gallos, J.P. Lemaistre, P. Argyrakis, *Chem. Phys.* **269**, 147 (2001)
- ¹⁸ K. Saito *et al.*, *J. Appl. Phys.* **69**, 8291 (1991); K. Saito, S. Honda, M. Watanabe, H. Yokoyama, *Jpn. J. Appl. Phys.* **33**, 6218 (1994); D.N. Krizhanovskii *et al.*, *J. Appl. Phys.* **93**, 5003 (2003)
- ¹⁹ P. Soven, *Phys. Rev.* **156**, 809 (1967); D.V. Taylor, *Phys. Rev.* **156**, 1017 (1967)
- ²⁰ R.J. Elliott, J.A. Krumhansl, P.L. Leath, *Rev. Mod. Phys.* **46**, 465 (1974)
- ²¹ D.L. Huber, W.Y. Ching, *Phys. Rev. B* **39**, 8652 (1989)
- ²² A. Boukahlil, D.L. Huber, *J. Lumin.* **45**, 13 (1990); **48/49**, 255 (1991)
- ²³ L.D. Bakalis, I. Rubtsov, J. Knoester, *J. Chem. Phys.* **117**, 5393 (2002)
- ²⁴ H. Shiba, *Progr. Theor. Phys.* **46**, 77 (1971)
- ²⁵ J.A. Blackman, D.M. Esterling, N.F. Berk, *Phys. Rev. B* **4**, 2412 (1971)
- ²⁶ D.M. Esterling, *Phys. Rev. B* **12**, 1596 (1975)
- ²⁷ A. Gonis, J.W. Garland, *Phys. Rev. B* **16**, 1495 (1977)
- ²⁸ K. Koepernik, B. Velický, R. Hayn, H. Eschrig, *Phys. Rev. B* **58**, 6944 (1998)
- ²⁹ D.A. Papaconstantopoulos, A. Gonis, P.M. Laufer, *Phys. Rev. B* **40**, 12196 (1989); K. Koepernik, B. Velický, R. Hayn, H. Eschrig, *ibid.* **55**, 5717 (1997); P.E.A. Turchi, D. Mayou, J.P. Julien, *ibid.* **56**, 1726 (1997); J.P. Julien, P.E.A. Turchi, D. Mayou, *ibid.* **64**, 195119 (2001)
- ³⁰ B.N.J. Persson, A. Liebsch, *Phys. Rev. B* **28**, 4247 (1983); B.N.J. Persson, *ibid.* **34**, 8941 (1986)
- ³¹ V.M. Rozenbaum, Yu.V. Skripnik, V.M. Ogenko, *Opt. Spectrosc.* **64**, 453 (1988)
- ³² F.J. Dyson, *Phys. Rev.* **92**, 1331 (1953); G. Theodorou, M.H. Cohen, *Phys. Rev. B* **13**, 4597 (1976); T.P. Eggarter, R. Riedinger, *ibid.* **18**, 569 (1978)
- ³³ As an example of the opposite behavior we can mention the nonexponential localization of the band-center wave function in a nearest-neighbor chain with off-diagonal disorder [see Ref. 34].
- ³⁴ G.G. Kozlov, V.A. Malyshev, F. Domínguez-Adame, A. Rodríguez, *Phys. Rev. B* **58**, 5367 (1998)
- ³⁵ *Langmuir-Blodgett Films*, ed. G. Roberts, Plenum Press, New York 1990
- ³⁶ A. Marletta *et al.*, *Macromolecules* **30**, 5729 (1997)